ACOUSTO-ULTRASONIC SOURCE INFLUENCE IN AN ANISOTROPIC LAYER

S. P. Pelts and J. L. Rose
Department of Engineering Science and Mechanics
Pennsylvania State University
114 Hallowell Building
University Park, PA 16802

INTRODUCTION

The current work addresses ultrasonic wave interaction within an orthotropic layer with two disk transducers in an acousto-ultrasonic mode. Earlier works have focused on studies of the influence of a rectangular transducer [1,2]. Acousto-ultrasonic techniques are useful in many cases where there is access to one side only. The different wave modes set-up in the layer are sensitive to many parameters such as source size, frequency, direction, etc. Computation of the wave structure within this layer of finite thickness is necessary to acquire quantitative information about material characterization and discontinuities. An attempt is made here to characterize the number and velocity of propagation modes with respect to direction and frequency. A special case of a composite is considered with particular values for azimuthal angle and frequency. Amplitude and velocity values for piston and parabolic source distributions have been calculated.

PROBLEM FORMULATION AND SOLUTION

Consider a linearly elastic orthotropic layer loaded on its upper surface by an axisymmetric distribution of normal surface traction in a circular region of radius r. The goal is to determine how the parameters of the various propagation modes depend on direction, frequency, structure, and how strongly each of the guided wave modes can be generated by such a source. Figure 1 shows the experimental setup to generate and receive propagation waves in the orthotropic plate using a transducer and receiver in an acousto-ultrasonic mode.

Review of Progress in Quantitative Nondestructive Evaluation, Vol. 14
Edited by D.O. Thompson and D.E. Chimenti, Plenum Press, New York, 1995

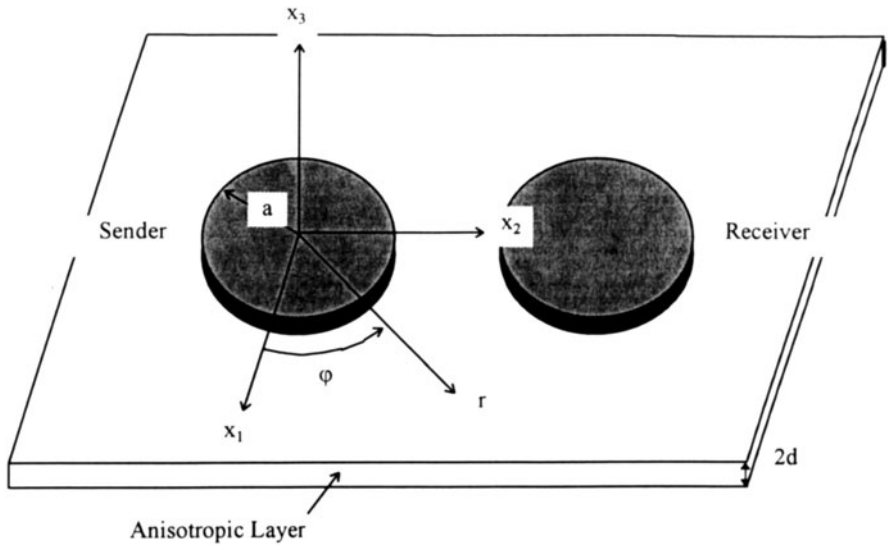

Figure 1. The acousto-ultrasonic experiment.

The equation of motion is given by

$$C_{ijkl}\frac{\partial^2 U_k}{\partial x_j \partial x_l} = \rho \frac{\partial^2 U_i}{\partial t^2} \tag{1}$$

where U_i is displacement, ρ is density and C_{ijkl} the elastic constants of the layer material. We can consider a decomposition of the elastic field into symmetric and antisymmetric parts as shown in Figure 2.

For the symmetric part, the elastic field must satisfy the following boundary conditions

$$\sigma_{33}(x_1, x_2, x_3 = \pm d, t) = \begin{cases} p(x_1, x_2)e^{-i\omega t} & \text{if } x_1^2 + x_2^2 \le a \\ 0 & \text{if } x_1^2 + x_2^2 > a \end{cases} \tag{2}$$

$$\tau_{31}(x_1, x_2, x_3 = \pm d, t) = \tau_{32}(x_1, x_2, x_3 = \pm d, t) = 0 \tag{3}$$

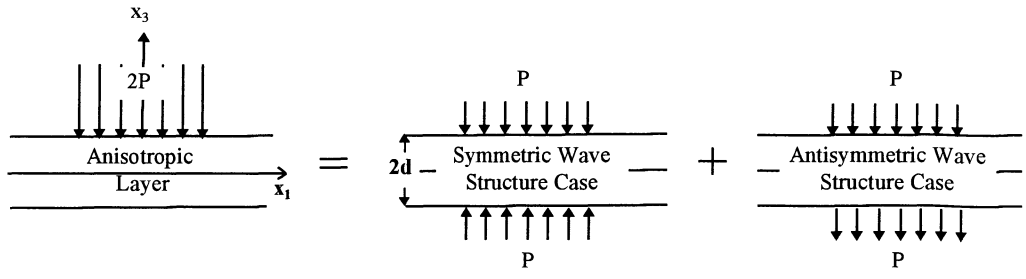

Figure 2. Decomposition of the elastic field into symmetric and antisymmetric parts.

where $p(x_1, x_2)$ is an arbitrary function which models the pressure distribution underneath the transducer face and ω is the circular frequency of the transducer. The solution for displacements can be written as

$$U_n(x_1, x_2, x_3, t) = u_n(x_1, x_2, x_3, t)e^{-i\omega t} \qquad (n=1,2,3) \quad (4)$$

Applying the two-dimensional Fourier integral transform to the equation of motion (1) and using the boundary conditions (2-3), we obtain formulas defining the displacements of the points in the layer. After this we superimpose the cylinder axis with the x_3 axis and locate the origin of coordinates on the middle face of the layer as shown in Figure 1. The displacements u_n of the layer can be written in the form

$$u_n(r,\varphi,x_3) = \frac{1}{4\pi^2}\int_0^{2\pi}\int_\Gamma K_n(\xi,\gamma,x_3,\omega)Q(\xi)e^{-i\xi r\cos(\varphi-\gamma)}\xi d\xi d\gamma \qquad (n=1,2,3;\ 0\le\varphi\le 2\pi) \quad (5)$$

$$x_1 = r\cos\varphi\ ,\ x_2 = r\sin\varphi \quad (6)$$

In the case of an axisymmetric load $p(r)$ we have

$$Q(\xi) = 2\pi\int_0^a p(\alpha)J_0(\xi\alpha)\alpha d\alpha \quad (7)$$

where $J_0(\xi\alpha)$ is a Bessel function. $K_n(\xi,\gamma,x_3,\omega)$ are the known functions with a finite set of real poles and a countable set of complex poles $\xi_m(\gamma)$. The poles are functions of the parameter γ. The integration contour Γ is chosen in accordance with radiation conditions. The properties of functions K_n and the contour of integration Γ were discussed in [3].

In order to illustrate the effects of the transducer radius and pressure distribution, consider a piston and parabolic type source of radius a, defined by (8) and (9).

$$\text{Piston} \qquad p(r) = \begin{cases} P & \text{if} \quad 0\le r\le a \\ 0 & \text{if} \quad r>a \end{cases} \quad (8)$$

$$\text{Parabolic} \qquad p(r) = \begin{cases} 2P[1-(r/a)^2] & \text{if} \quad 0\le r\le a \\ 0 & \text{if} \quad r>a \end{cases} \quad (9)$$

The resultant force is the same in both cases. Calculating in Eq.(5) the residues of the integrands in the real poles intersected by the deformed contour Γ and applying the method of stationary phase, we obtain in the far-field the following asymptotic approximation for the displacement vector components.

$$u_n(r,\varphi,x_3) \approx d\sum_m A_{nm}(\varphi,x_3,\omega)\frac{e^{ik_m(\varphi)r}}{\sqrt{r}} \qquad (n = 1,2,3) \qquad (10)$$

The wavenumber k_m is a function of φ and the material properties while $A_{mm}(\varphi,x_3,\omega)$ depends on the material properties and properties of the source used for excitation. Hence the phase velocity of the propagation modes,

$$V_{ph}^{m} = \frac{\omega}{k_m(\varphi)} \qquad (11)$$

can be calculated in various directions. Some numerical results for the symmetric wave structure for an example composite with density 1.447 g/cm ^{3} and elastic constants given in Table 1 are shown in Figures 3-6. The modes in Figure 3 are numbered according to the wave number k_m which are the roots of the dispersion equation.

Table 1. Elastic constants for an example composite.

C_{11}	C_{12}	C_{13}	C_{22}	C_{23}	C_{33}	C_{44}	C_{55}	C_{66}
79.23	5.84	3.47	71.35	3.41	8.15	4.13	4.12	5.39

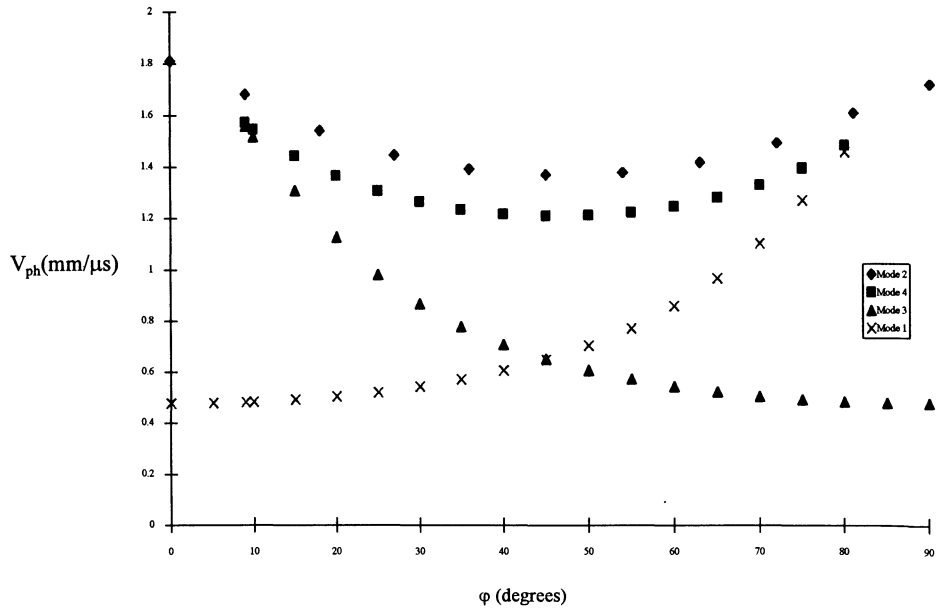

Figure 3. Phase velocity V_{ph} values vs. azimuthal angle φ in orthotropic plate.

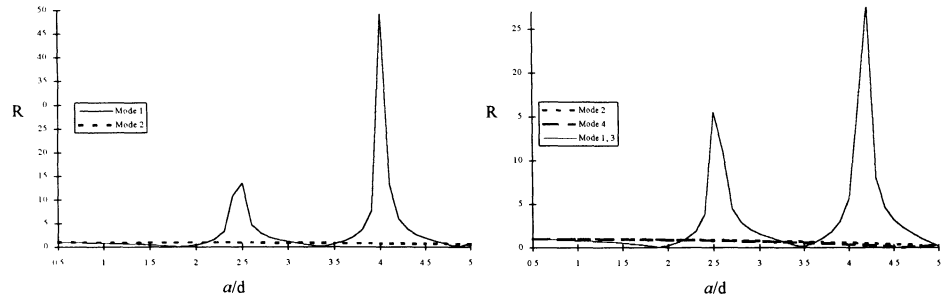

Figure 4. Examples of magnitude ratio $R = \left| u_{i\ piston} / u_{i\ parabolic} \right|$ $(i = 1,2,3)$ vs. a/d for two cases of (a) $\varphi = 0$ and (b) $\varphi = 45$ when $\omega d = 1$.

Figure 4 is the absolute ratio of wave amplitude from piston source to that from parabolic source showing the effect of the source type on the wave distribution. Figure 5 is the enlarged lower part of Figure 4, showing the small differences between the modes.

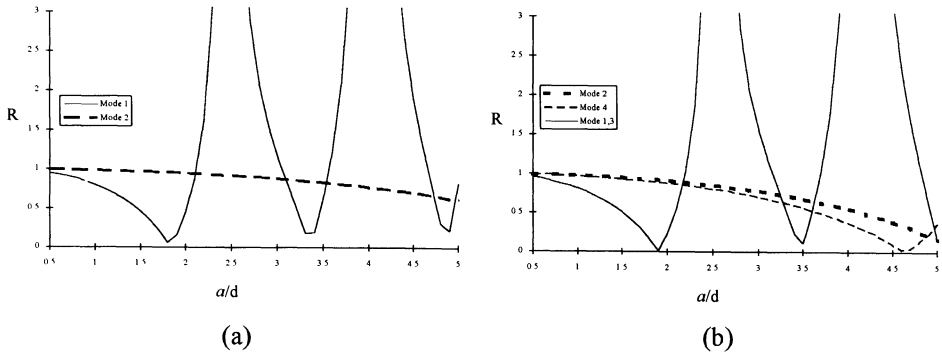

Figure 5. The relation of Figure 4(a, b) in a different scale with modes 1,2,3,4 labeled as shown.

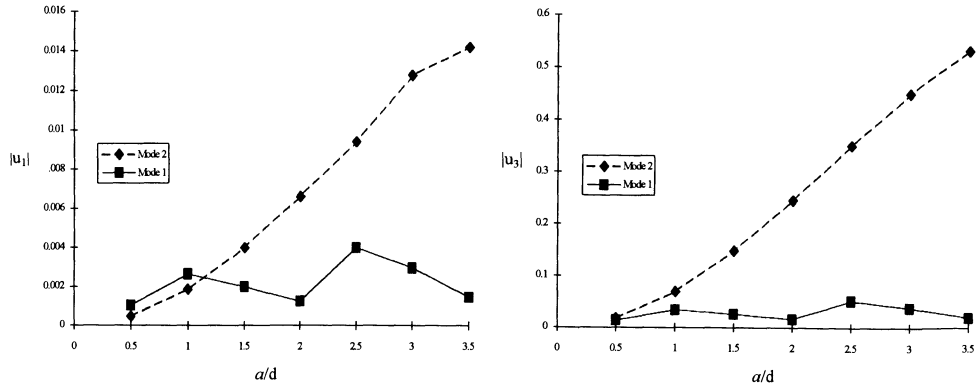

Figure 6. Calculated non-dimensional amplitudes $|u_1|$ and $|u_3|$ for a piston source, when $\varphi = 0$, $\omega d = 1$.

CONCLUDING REMARKS

For an orthotropic layer, the number and velocity of the propagation modes depends on the direction and frequency. Amplitudes of some of the propagation modes depend strongly on the pressure distribution. The first mode is found to be most sensitive to changes in the pressure distribution. Amplitudes of the propagation modes depend on the size of the transducer.

ACKNOWLEDGMENT

The authors would like to thank Alex Vary of the NASA Lewis Research Center for discussions and support.

REFERENCES

1. J. L. Rose, J. J. Ditri and A. Pilarski, "Source influences on the excitation of guided elastic waves in anisotropic layers," Proceedings of the ninth international conference on composite materials. (ICCM/9), Madrid, Spain, Vol. VI edited by A. Miravete (University of Zaragoza, Woodhead Publishing Limited, 1993), pp. 811-818.
2. J. L. Rose, J. J. Ditri and A. Pilarski, "Wave mechanics principles in acousto-ultrasonic NDE," Proceedings of the second international conference on acousto-ultrasonics Topical conference, Atlanta, GA, edited by A. Vary (The American Society for Nondestructive Testing, Inc. 1993), pp. 21-28.
3. V. A. Babeshko, Sov. Phys. Dokl. 23(9), pp. 685-687 (1978).